

# ISW-Galaxy Cross Correlation: A probe of Dark Energy clustering and distribution of Dark Matter tracers

Shahram Khosravi,<sup>1,\*</sup> Amir Mollazadeh,<sup>1</sup> and Shant Baghran<sup>2,3,†</sup>

<sup>1</sup>*Department of Physics, Kharazmi University, Tehran, Iran*

<sup>2</sup>*Department of Physics, Sharif University of Technology, P. O. Box 11155-9161, Tehran, Iran*

<sup>3</sup>*School of Astronomy, Institute for Research in Fundamental Sciences (IPM), P. O. Box 19395-5531, Tehran, Iran*

The Integrated Sachs Wolfe (ISW) cross correlation with the galaxy distribution in late time is a promising tool to constrain the dark energy properties. In this work we study the effect of dark energy clustering on the ISW-galaxy cross correlation. Indicating the fact that the bias parameter between the distribution of the galaxies and the underlying dark matter introduce a degeneracy and complications. We argue that as the time of the galaxy's host halo formation is different from the observation time, we have to consider the evolution of the halo bias parameter. We indicate that any deviation from  $\Lambda$ CDM model will change the evolution of the bias as well. Also we show that the halo bias strongly depends on the sub-sample of galaxies which is chosen for cross correlation. We show that joint kernel of ISW effect and the galaxy distribution have the dominant effect on the observed signal, accordingly we can enhance the signal of a specific dark energy model by choosing an appropriate tracer. More specifically we compare the clustered dark energy models with two samples of galaxies. First is a sub-sample of galaxies from Sloan Digital chosen with the r-band magnitude  $18 < r < 21$  with a host dark matter halos of mass  $M \sim 10^{12} M_{\odot}$  and formation redshift of  $z \sim 2.5$ . Secondly with the sub-sample of Luminous Red galaxies with a host dark matter halos of mass  $M \sim 10^{13} M_{\odot}$  and formation redshift of  $z \sim 2.0$ . Using the evolved bias we improve the  $\chi^2$  for the  $\Lambda$ CDM which it reconcile the  $\sim 1\text{-}2\sigma$  tension of the ISW-galaxy signal and  $\Lambda$ CDM prediction. Finally we show how sub-samples change the bias parameter and will improve the constraints on dark energy clustering.

## I. INTRODUCTION

For more than a decade there is a considerable amount of evidence for the accelerated expansion of the Universe. The Hubble-diagram of type Ia Supernova indicates that the  $\sim 70\%$  of the Universe is made of unknown component, dark energy, that accelerates the expansion of the Universe [1, 2]. The angular power spectrum of Cosmic Microwave Background (CMB) radiation measured by WMAP [3] and Planck [4], also shows that the spatial curvature of the Universe is almost flat and dark energy is needed to explain the CMB temperature fluctuation's power spectrum. On the other hand, the Large scale structure (LSS) surveys map the distribution of the galaxies in different redshifts and different angular scales. The statistical properties of their distribution also indicates that the dark energy plays a major role [5].

Due to the observational indication of the existence of dark energy, there is a tremendous amount of literature trying to explain the accelerated expansion of the Universe, mainly categorized in three groups of solutions. 1) The Cosmological Constant (CC) [6] 2) The modification of the gravity (MG) [7–10] and 3) the Dark energy (DE) models [11]. Accordingly the cosmological observations that can discriminate between the above solutions become very important [12–14]. The detection of Baryon Acoustic Oscillations (BAO) in matter power spectrum [15–18], the observation of the cluster of the galaxies [19], the cosmic shear [20] and Lyman alpha forest [21] are among the important and promising observations for cosmological studies. Beside these observations, the Integrated Sachs-Wolfe (ISW) [22] is a new direction in observational cosmology in order to constrain the cosmological models [23, 24].

In this work, we study the effect of the clustered dark energy models as possible extension of the smooth dark energy quintessential like models on ISW effect. We proposed that the ISW is a promising tool to detect the clustering effect. However due to the cosmic variance effect, the ISW signal can be detected via its cross correlation with the late time tracers of dark matter distribution [25–29]. We investigate this effect and we show that there is a degeneracy between the dark energy fluid properties and the bias parameter which relates the clustering of galaxies to the underlying distribution of dark matter. Also we show the effect of the distribution of dark matter tracers (galaxies) on the ISW-

---

\*Electronic address: khosravi-AT-ipm.ir

†Electronic address: baghran-AT-sharif.edu

galaxy signal. We conclude that the bias parameter and a joint kernel function that encapsulates the effect of the galaxy distributions change the effectiveness of a dark energy in different redshifts. We also study the theoretical ISW-galaxy power spectrum using the evolved bias parameter and we investigate the situation of the compatibility of models with observation data. The future surveys can constrain the dark energy parameters better and we also need complimentary observations that can break the degeneracy of bias and dark energy clustering and an appropriate sample of galaxies to probe the effect of dark energy in a specific redshift. The structure of this work is as below: In Sec.(II) we review the theoretical background for the "Integrated Sachs Wolfe-galaxy" (ISW-g) cross correlation. In Sec.(III) we study the clustering of dark energy models and their effect on the ISW-g signal. In Sec. (IV) we study the bias and review the concept of the evolving bias parameter. In Sec. (V) we present our results on the ISW-g cross correlation with two samples of galaxies (Luminous Red galaxies (LRG) and Sloan Digital Sky survey(SDSS) magnitude chosen galaxies) for different dark energy models and different biases and finally in Sec.(VI) we have the conclusion and future remarks.

## II. THE ISW- GALAXY CROSS CORRELATION

In this section we review the theoretical background for the ISW-galaxy correlation signal and its relation to the dark matter power spectrum. In order to study the effect of gravitational perturbations on the CMB photons, we use the perturbed FRW-metric in Newtonian gauge as:

$$ds^2 = -[1 + 2\Psi(\mathbf{x}, t)]dt^2 + [1 + 2\Phi(\mathbf{x}, t)]a^2(t)dx^i dx_i \quad (1)$$

where  $\Psi$  and  $\Phi$  are scalar metric perturbations. In the framework of General relativity(GR) and the assumption that the cosmic fluid has no anisotropic stress term in its energy-momentum tensor, then we will have  $\Psi = -\Phi$ . The Integrated Sachs Wolfe (ISW) is the imprint of the gravitational potential change on the temperature of the photons free streaming from the last scattering surface. In the matter dominated era the gravitational potential is almost constant, however when the Universe enters the phase of dark energy dominated era the potential gradually become shallower and shallower. The time dependence of the gravitational potential introduce an effect on temperature perturbations of CMB photons as they fall and come out of the potential well which are not constant. This effect is related to the matter potential change as below [30]:

$$\left(\frac{\Delta T}{T}\right)_{ISW}(\theta_x, \theta_y) = - \int_{\eta_i}^{\eta_0} d\eta e^{-\tau} \frac{\partial \psi(\vec{\theta})}{\partial \eta} = \sum_{lm} a_{lm}^T Y_{lm}(\hat{n}) \quad (2)$$

where temperature anisotropy is a function of 2D position  $\hat{n} = (\theta_x, \theta_y)$ ,  $\eta$  is the conformal time, and the integral is taken from some pre-recombination epoch  $\eta_i$  to the present time  $\eta_0$  and  $\tau$  is the optical depth. The second equality comes from the spherical harmonic expansion of temperature change and  $a_{lm}^{(T)}$  is the expansion coefficients. Note that  $\psi$ (ISW potential) is defined as:

$$\psi(\mathbf{x}, t) = \Phi(\mathbf{x}, t) - \Psi(\mathbf{x}, t) \quad (3)$$

Worth to mention that the ISW effect and the weak gravitational lensing are prominent observations that probe both scalar perturbed quantities in geometrical section( $\Psi$  and  $\Phi$ ), while the dynamical motion of dark matter tracers and Poisson equation are sensitive to one of the potentials correspondingly. The optical depth  $\tau$  is a line of site integral of the number density of free electrons  $n_e$  times the Thompson scattering cross section  $\sigma_T$  as below:

$$\tau = \int_{\eta_i}^{\eta_0} n_e \sigma_T d\eta \quad (4)$$

where the integral is taken from the time of the last scattering surface to present time. In this work we will neglect the optical depth. Now we can Fourier transform the ISW potential and write the integrals hereafter in terms of redshift:

$$\left(\frac{\Delta T}{T}\right)_{ISW}(\hat{n}) = \int \frac{d^3 k}{(2\pi)^3} \int_{z_0}^{z_{CMB}} dz \frac{\partial}{\partial z} \left( e^{i\vec{k} \cdot \vec{r}} \psi_k \right) \quad (5)$$

where  $\psi_k$  is the Fourier transform of ISW potential. In the framework of GR and with assumption of cosmic fluid with no anisotropic term in its energy-momentum tensor, the ISW potential is related to matter density in dark matter dominated era as:

$$\psi = \frac{3H_0^2 \Omega_m^0}{k^2} \frac{D(z)}{D(z=0)} (1+z) \delta_m^{(0)} \quad (6)$$

where  $\delta_m^{(0)}$  is present day matter density perturbation,  $\Omega_m^0$  is the present day density parameter,  $D(z)$  is the growth function of dark matter perturbations normalized to its value in  $z = 0$  and  $H_0$  is the present value of Hubble constant. In order to study the properties of dark energy, two important points leads us to use the cross correlation of ISW and galaxy distribution. 1) The cosmic variance put limitations on the accuracy of ISW effect as a cosmic probe. Accordingly the signal can be extracted by using the cross correlation technique with late time tracers of dark matter distribution like the distribution of the galaxies. 2) The ISW effect is obtained from time evolution of gravitational potentials and due to Poisson equation the same potential wells that cause the ISW effect are related to the dark matter distribution. In this light, we can study the dark energy and its effect on ISW signal via the cross correlation of the temperature change of CMB with the distribution of matter as first proposed by [25].

The matter distribution along the line of sight can be projected in two dimensions as:

$$\delta(\theta_x, \theta_y) = \int dz \frac{dN}{dz} \delta_m(z) = \sum_{lm} a_{lm}^{(g)} Y_{lm}(\hat{n}) \quad (7)$$

where  $\delta_m(z)$  is the three dimensional matter density contrast, and  $dN/dz$  is the selection function which encapsulate in it the distribution of the galaxies observed by a survey. In the second equality we expand the two dimensional field of the density contrast in spherical harmonics and  $a_{lm}^{(g)}$  is the coefficient of the expansion. Now we can calculate the angular power spectrum of cross correlation of the expansion coefficients of ISW temperature change and galaxy distribution as below:

$$C_\ell^{gT} = \frac{2}{\pi} \int_0^\infty k^2 dk I_\ell^{ISW}(k) I_\ell^g(k) P_m^{(0)}(k) \quad (8)$$

where  $C_\ell^{gT} \equiv \langle a_{\ell m}^{(g)} a_{\ell m}^{(T)} \rangle$  and  $P_\delta^{(0)}(k)$  is the matter power-spectrum in present time.  $I_\ell^{ISW}$  and  $I_\ell^g$  each represent the specific kernel function of the ISW and galaxy distribution, which relates the the matter density power spectrum to the angular power of the cross correlation. Each of the specific kernels are obtained as below respectively:

$$I_\ell^{ISW}(k) = \frac{3H_0^2 \Omega_{m,0}}{k^2} \int dz \frac{d}{dz} (D(z)(1+z)) j_\ell[k\chi(z)] \quad (9)$$

$$I_\ell^g(k) = \int dz b(k, z) \frac{dN}{dz} D(z) j_\ell[k\chi(z)] \quad (10)$$

where  $D(z) \equiv \delta(z)/\delta(0)$  is the growth function.  $dN/dz$  is normalized such as  $\int dz \frac{dN}{dz} = 1$ .  $j_\ell$  are the spherical Bessel which depends on the comoving distance  $\chi$ .  $b(k, z)$  is the bias parameter which in general is a scale and redshift dependent quantity and it relates the density contrast of the dark matter to the density contrast of the galaxy distribution. The dynamic of the dark energy and any deviation from standard  $\Lambda$ CDM can change the angular power through the growth function. Also the relation between the gravitational potential and the matter distribution may be modified in non  $\Lambda$ CDM models. In the next Sec.(III), we will study the effect of the clustered dark energy on the signal. On the other hand the bias parameter introduces another uncertainty beside the cosmological model. The precise determination of the galaxy bias may help to underpin any deviation from standard  $\Lambda$ CDM prediction. In Sec.(IV) we will discuss the theoretical aspects of the bias.

### III. DARK ENERGY CLUSTERING AND ISW EFFECT

In this section we discuss the extension of the smooth dark energy models to the clustered ones. We will show how the dark energy clustering will change the ISW-g cross correlation through the modified poisson equation. The dark energy can be considered as a cosmological fluid with a general energy-momentum tensor as below:

$$T_{\mu\nu} = (\rho + P)u_\mu u_\nu + P g_{\mu\nu} + q_\mu u_\nu + q_\nu u_\mu + \pi_{\mu\nu} \quad (11)$$

where  $\rho$  and  $P$  are the density and pressure of the fluid,  $u_\mu$  is the four velocity,  $q_\mu$  is heat transfer vector and  $\pi_{\mu\nu}$  is the viscous shear tensor. First we assume that the heat transfer and the viscous shear tensor for the dark energy fluid is zero. However we relax the assumption that the dark energy is a smooth fluid with Jeans length equal to horizon. Accordingly the fluid can be described by the equation of the state  $w$  and sound speed of the fluid  $c_s$  which will be introduced in below. The equation of state  $w = P/\rho$  in general can be a redshift dependent quantity while

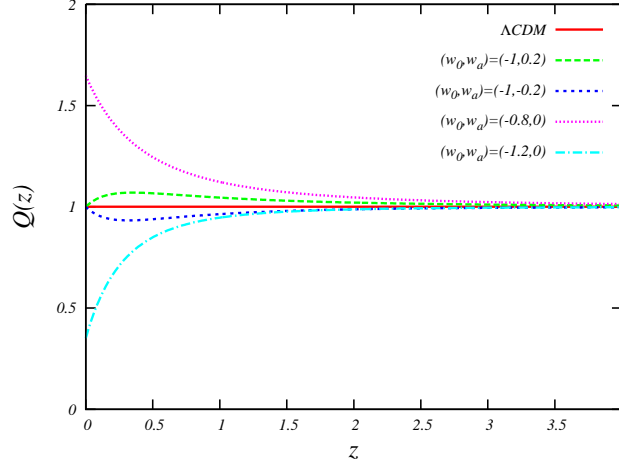


FIG. 1: The function  $Q$  is plotted versus redshift for different models of dark energy. The red solid line indicate the  $\Lambda$ CDM, the green long-dashed line shows a dark energy model with  $(w_0, w_a) = (-1, 0.2)$  in CPL parameterizations. The blue dashed line is for a model with  $(w_0, w_a) = (-1, -0.2)$ . The magenta dotted line is for equation of state  $(w_0, w_a) = (-0.8, 0)$  and cyan dashed-dotted line indicate  $(w_0, w_a) = (-1.2, 0)$ .

the cosmological constant with equation of state  $w = -1$  is a special case of dark energy fluid. In order to define the sound speed, we consider the fact that the pressure of the fluid can be a function of density and entropy both, ( $P = P(\rho, S)$ ), accordingly:

$$c_s^2 = \frac{\delta P(\rho, S)}{\delta \rho} = \frac{\partial P}{\partial \rho}|_S + \frac{\partial P}{\partial S}|_\rho \frac{\partial S}{\partial \rho} = c_{s(a)}^2 + c_{s(na)}^2 \quad (12)$$

where  $c_{s(a)}^2$  is the adiabatic sound speed and  $c_{s(na)}^2$  is the non-adiabatic sound speed of the fluid. For simplicity we assume that  $c_{s(na)}^2 = 0$ . In this work the extension of the dark energy clustering models with respect to the smooth dark energy models comes from the adiabatic sound speed term. In this case, if the sound speed is not equal to unity, it means that the Jeans length of dark energy perturbations would be smaller than the horizon. This means that we anticipate dark energy clusters in sub-horizon scales which will have an effect on the evolution of dark matter through the field equations. Now we can find the perturbed energy-momentum tensor terms via [30]:

$$\delta T_\nu^\mu = \rho[\delta(1 + c_s^2)u_\nu u^\mu + (1 + w)(\delta u_\nu u^\mu + u_\nu \delta u^\mu) + \delta_\nu^\mu c_s^2 \delta] \quad (13)$$

and replace it in perturbed Einstein equations  $G_\nu^\mu = 8\pi G \delta T_\nu^\mu$ , where  $\delta$  is the density contrast. Beside the field equations the energy-tensor conservation  $T_{\nu;\mu}^\mu = 0$  for two cosmic fluids, dark matter and dark energy, results in continuity and Euler equation in Fourier space as below:

$$\begin{aligned} \delta'_m + \theta_m + 3\Phi' &= 0 \\ \theta'_m + \mathcal{H}\theta_m - k^2\Psi &= 0 \\ \delta'_{de} + 3\mathcal{H}(c_s^2 - w)\delta_{de} + (1 + w)(\theta_{de} + 3\Phi') &= 0 \\ \theta'_{de} + [\mathcal{H}(1 - 3w) + \frac{w'_{de}}{1 + w_{de}}]\theta_{de} - k^2(\frac{c_s^2}{1 + w}\delta_{de} + \Psi) &= 0 \end{aligned} \quad (14)$$

where  $\delta_m$  and  $\delta_{de}$  are the dark matter and dark energy density contrast,  $\theta_m$  and  $\theta_{de}$  are the Fourier transform of the divergent of each fluids velocity.  $\mathcal{H} = aH$  is the conformal Hubble parameter and the prime is derivative with respect to conformal time. Note that  $w$  and  $c_s$  are the equation of state and sound speed of dark energy. In order to study the distribution of matter in large scales we have to find the time evolution of dark matter density. However the presence of dark energy and its properties effect the dynamic and distribution of dark matter through Hubble parameter and the gravitational potential. The gravitational potential is related to the two fluids perturbed parameters via Poisson equation as below:

$$k^2\Phi = 4\pi G a^2 \rho_m [\delta_m + \frac{3\mathcal{H}}{k^2}\theta_m + \frac{\rho_{de}}{\rho_m}(\delta_{de} + 3(1 + w)\frac{\mathcal{H}}{k^2}\theta_{de})] \quad (15)$$

In the sub-horizon limit the Poisson equation can be written approximately as:

$$k^2 \Phi \simeq 4\pi G \rho_m a^2 \delta_m Q \quad (16)$$

where  $Q$  is defined as below:

$$Q = 1 + \frac{\rho_{de} \delta_{de}}{\rho_m \delta_m} \quad (17)$$

In the smooth dark energy models where  $\delta_{de} = 0$  the  $Q = 1$ , we will recover the standard case. Any deviation of parameter  $Q$  from unity will be an indication of a deviation from  $\Lambda$ CDM. Now in order to solve for the dynamics of density contrast, we also assume that the fluid is barotropic, accordingly the sound speed is related to equation of state as below:

$$c_s^2 = w - \frac{w'}{3\mathcal{H}(1+w)} \quad (18)$$

For our case of study we use the Chevallier-Polarski-Linder (CPL) parametrization of the dark energy as [31, 32]:

$$w_{de}(z) = w_0 + w_a \left( \frac{z}{1+z} \right) \quad (19)$$

where  $w_0$  and  $w_a$  are free parameters. In the case of  $(w_0, w_a) = (-1, 0)$  we will recover the  $\Lambda$ CDM case.

In Fig.(1), we plot the  $Q$  versus redshift for different models of dark energy with CPL equation of state. The solid redline shows the  $\Lambda$ CDM where  $Q = 1$  and we do not have any deviation from the standard case. The  $Q(z)$  is plotted for set of equation of states with free parameters  $w_0$  and  $w_a$  defined as a set of  $(w_0, w_a) = \{(-1, 0.2), (-1, -0.2), (-0.8, 0), (-1.2, 0)\}$ . The  $Q$  in Eq.(16) shows how the Poisson equation is modified.  $Q > 1$  ( $Q < 1$ ) indicates that the same amount of matter perturbation produces more (less) gravitational potential with respect to  $\Lambda$ CDM. Intuitively we anticipate that  $Q > 1$  ( $Q < 1$ ) enhances (diminishes) the amplitude of the ISW-g signal which is related to the matter power spectrum. In the next Section, we will show that this is not always the case and in order to study the effect of the dark energy on the observable quantities we have to know about the tracers of the dark matter distribution as well.

In the next step, we have to solve the dynamical equation for the matter density:

$$\delta_m'' + \mathcal{H} \delta_m' + k^2 \Psi + (3\mathcal{H} \Phi' + 3\Phi'') = 0 \quad (20)$$

worth to mention that the last term in parentheses can be neglected due to quasi static approximation, also the  $k^2 \Psi$  is related to the dark matter and dark energy density contrast through Eq.(16). In the Sec.(V), for our theoretical estimation of matter power spectrum we use the solution of Eq.(20) to extract the growth function of matter distribution in extended dark energy models and plug it in the power spectrum defined as below:

$$P_m(k, z) = A k^{n_s} T^2(k) D^2(z) \quad (21)$$

where  $D(z)$  is the growth function obtained from solving Eq.(20). The evolution of potential with respect to scale is introduced in transfer function  $T(k)$ . In this work we use the Bardeen, Bond, Kaiser, Szalay (BBKS) transfer function [33].  $A$  and  $n_s$  are the amplitude and the spectral index of perturbations. The final and very important point to indicate here is that in the ISW-g cross correlation, we need to know the power-spectrum of galaxy distribution. Also the specific kernel of ISW-g effect will change as below accordingly:

$$\tilde{I}_\ell^{ISW}(k) = \frac{3H_0^2 \Omega_{m,0}}{k^2} \int dz \frac{d}{dz} (\tilde{D}(z)(1+z)Q(z)) j_\ell[k\chi(z)] \quad (22)$$

$$\tilde{I}_\ell^g(k) = \int dz b(k, z) \frac{dN}{dz} \tilde{D}(z) j_\ell[k\chi(z)] \quad (23)$$

where  $\tilde{\phantom{x}}$  indicate the modified kernels due to models that deviates from  $\Lambda$ CDM. Accordingly we must know the relation of the galaxies distribution with respect to the dark matter. In the next section we will discuss the bias of matter and galaxies and we will show how the dark energy models change the evolved bias parameter as well.

#### IV. THE EFFECT OF COSMOLOGY ON DARK MATTER HALO BIAS

In this section we will discuss the relation of the galaxy distribution with the underlying dark matter. This is a very important issue in cosmological studies as the theoretical models predicts the distribution and the growth of dark matter perturbations, while the observations are done with luminous matter (like galaxies). The density contrast of galaxy distribution and the underlying dark matter distribution is related via bias parameter. The bias parameter in general can be a scale and redshift dependent quantity  $b(z, k)$ . The halo bias parameter relates the distribution of dark matter halos with respect to dark matter distribution, on the other hand the galaxy bias will depend on the Halo Occupation Distribution (HOD) and indicate that in a halo of a desired mass  $M$ , how many galaxies with Luminosity  $L$  is there [34]. The theoretical study and the observational investigation is needed to pin down the bias parameter. This is important in its own nature to study the processes of structure formation. The study of the physics of bias is important because it introduces uncertainties in cosmological data interpretation. And there will be a probable degeneracy between the bias parameter and the deviation from  $\Lambda$ CDM model [13].

In this work, we show and quantify the amount of uncertainty, which is introduced by bias parameter. In this light, we will mainly focus on the halo bias term and we assume that the galaxy bias is almost one. The halo bias which can be defined as the number density contrast of halos  $n(M, z)$  in the presence of long mode dark matter distribution  $\delta_l$  defined as:

$$b(k, z) = \delta_h / \delta_m = \left( \frac{n(M, z; \delta_l) - \bar{n}(M, z)}{\bar{n}(M, z)} \right) / \delta_m \quad (24)$$

where  $\bar{n}(M, z)$  is the number density of structures when long mode perturbation is set to zero, and also we set the long mode density contrast equal to the matter density contrast in linear regime  $\delta_m$ . The bias parameter in its simplest definition is just related to the mass of dark matter halo which hosts the observed galaxies. The Press-Schechter bias parameter from the peak background splitting method in Eulerian frame is obtained as [35]:

$$b_{PS}^E(M; z) = 1 + \frac{\nu^2(M, z) - 1}{\delta_c} \quad (25)$$

where  $\delta_c$  is the critical density of spherical collapse and  $\nu$  is the height parameter defined as  $\nu = \delta_c / \sigma(M)$ , where  $\sigma(M)$  is the variance of density perturbation in a window function related to the mass  $M$ . It is worth to mention that the number density of structures is linked to the underlying cosmological model via the matter density variance. In the Press-Schechter formalism the bias parameter first calculated in Lagrangian formalism and there is a hidden assumption that the formation time of a dark matter halo and the observation time is the same. However that is not quite right and always there is a difference between the formation and observation redshift.

Now in the case that we are probing the possible deviation from  $\Lambda$ CDM we must note that the bias parameter evolved differently from formation time up to observation time in different cosmological models. Accordingly the bias parameter must be considered consistently with the model we chose. In order to study the effect of evolution of bias parameter from formation to observation we study this evolution using the continuity and Euler equation for dark and luminous matter [36–38]. Using Einstein equations in the level of perturbation it can be shown that the governing equations for underlying Dark Matter of the universe are:

$$\delta'_m = -\nabla \cdot [(1 + \delta_m) \mathbf{v}_m] \quad (26)$$

$$\mathbf{v}'_m + (\mathbf{v}_m \cdot \nabla) \mathbf{v}_m + \frac{a'}{a} \mathbf{v}_m = -\nabla \phi \quad (27)$$

$$\nabla^2 \phi = 4\pi G \bar{\rho}_m a^2 \delta_m. \quad (28)$$

where  $\mathbf{v}_m$  is the peculiar velocity of matter,  $\phi$  is the gravitational potential which can be traced back to metric perturbations and by  $'$  we mean the derivative with respect to conformal time. On the other hand, the dynamic of galaxies as point-like particles obey the following equations accordingly:

$$\delta'_g = -\nabla \cdot [(1 + \delta_g) \mathbf{v}_g] \quad (29)$$

$$\mathbf{v}'_g + (\mathbf{v}_g \cdot \nabla) \mathbf{v}_g + \frac{a'}{a} \mathbf{v}_g = -\nabla \phi \quad (30)$$

$$(31)$$

where  $\delta_g = (n_g - \bar{n}_g) / \bar{n}_g$  is the galaxy over-density. ( $n_g$  is the galaxy number density and  $\bar{n}_g$  is the spatial average of it.)  $\mathbf{v}_g$  is the peculiar velocities of galaxies. An important point to indicate here is that the continuity and Euler equation



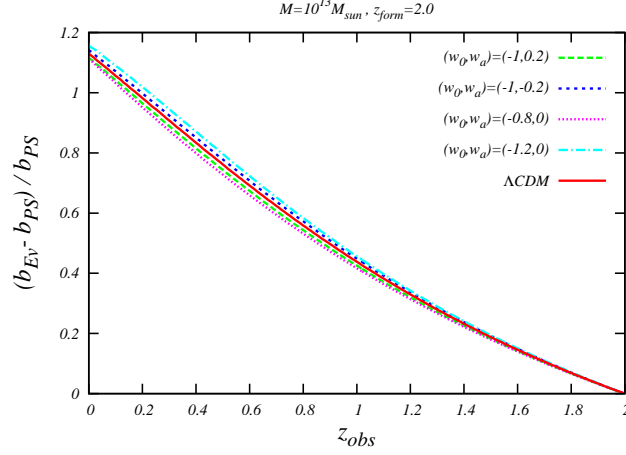


FIG. 2: The ratio of Evolved bias to Press Schechter bias minus one is plotted versus the observation redshift for different models of dark energy. The red solid line indicate the  $\Lambda$ CDM, the green long-dashed line shows a dark energy model with  $(w_0, w_a) = (-1, 0.2)$  in CPL parameterizations. The blue dashed line is for a model with  $(w_0, w_a) = (-1, -0.2)$ . The magenta dotted line is for equation of state  $(w_0, w_a) = (-0.8, 0)$  and cyan dashed-dotted line indicate  $(w_0, w_a) = (-1.2, 0)$ . The dark matter halo is assumed to have a mass of  $M = 10^{13} M_\odot$  as a typical mass of a SDSS LRG catalog galaxies host with formation redshift  $z_{form} = 2.0$ .

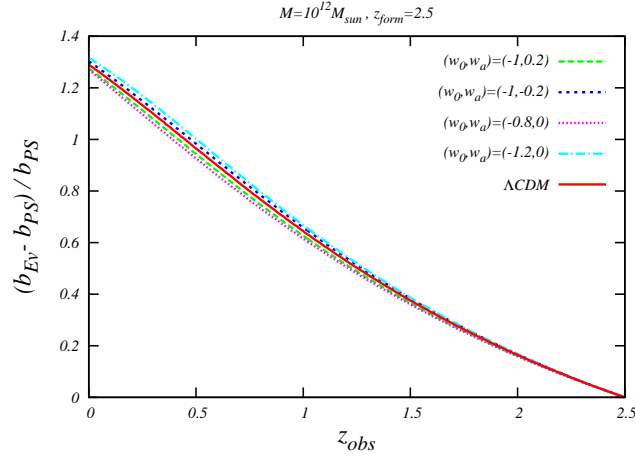


FIG. 3: The ratio of Evolved bias to Press Schechter bias minus one is plotted versus the observation redshift for different models of dark energy. The red solid line indicate the  $\Lambda$ CDM, the green long-dashed line shows a dark energy model with  $(w_0, w_a) = (-1, 0.2)$  in CPL parameterizations. The blue dashed line is for a model with  $(w_0, w_a) = (-1, -0.2)$ . The magenta dotted line is for equation of state  $(w_0, w_a) = (-0.8, 0)$  and cyan dashed-dotted line indicate  $(w_0, w_a) = (-1.2, 0)$ . The dark matter halo is assumed to have a mass of  $M = 10^{12} M_\odot$  as a typical mass of a SDSS galaxy catalog galaxies host with formation redshift  $z_{form} = 2.5$ .

of dark matter and galaxies have the same form with respect to their perturbed quantities while the gravitational potential  $\phi$  in contrast is exactly the same value which is mainly sourced by the dark matter distribution. Using the equations above one can show that

$$(\mathbf{v}_g - \mathbf{v}_m)' + \frac{a'}{a}(\mathbf{v}_g - \mathbf{v}_m) = 0. \quad (32)$$

which can be written as  $(\mathbf{v}_g - \mathbf{v}_m) \propto \frac{1}{a}$ .

The velocity difference in principle can be a position dependent pre-factor. By assuming that matter and galaxies experience the same gravitational potential we find that  $\mathbf{v}_g = \mathbf{v}_m$ . In other words even if there was a bias between the  $\mathbf{v}_g$  and  $\mathbf{v}_m$  initially, it will be washed away eventually. Following the same logic, The difference of density contrasts

of galaxy and bias will like:

$$(\delta_g - \delta_m)' = -\nabla \cdot (\mathbf{v}_g - \mathbf{v}_m) \equiv -\frac{1}{a} \nabla \cdot \mathbf{u}_0, \quad (33)$$

where  $\mathbf{u}_0$  is a function of position alone and not time. The integration of Eq.(33) results

$$\delta_g - \delta_m = -\nabla \cdot \mathbf{u}_0 \int \frac{da}{a^3 H} + \Delta_i. \quad (34)$$

The first term in the above equation is a decaying term, so it will have no importance in our discussion whatsoever. The second term  $\Delta_i$  plays the crucial role. ( $i$  indicates to the initial time). So the bias parameter will evolve as

$$b(a) \equiv \frac{\delta_g(a)}{\delta_m(a)} = 1 + \frac{\Delta_i}{\delta_m(a)}. \quad (35)$$

As we mentioned  $\Delta_i$  is time-independent so we can write it as follow

$$\Delta_i = (b_i - 1)\delta_m(a_i) \quad (36)$$

where  $b_i$  and  $\delta_m$  has been evaluated at some initial time. Now, assuming that the galaxy bias is initially scale dependent we can show that in Fourier space:

$$b(a, k) = 1 + (b_i - 1) \frac{\delta_m(a_i, \mathbf{k})}{\delta_m(a, \mathbf{k})} \quad (37)$$

Now we can exchange the ratio of the density contrasts with growth function  $D(k, z)$ , which in cosmological models, which deviates from  $\Lambda$ CDM model can be scale dependent as well. Now the bias in observed redshift  $z_{obs}$  can be related to the Lagrangian bias computed in the formation redshift  $z_{form}$  as below (so we set the initial time to the formation time):

$$b_{Ev}(k_0, z_{obs}; z_{form}) = 1 + [b_{PS}(z_{form}) - 1] \frac{D(k_0, z_{form})}{D(k_0, z_{obs})} \quad (38)$$

where  $b_{Ev}$  is the evolved bias and  $b_{PS}$  is the Press-Schechter bias in formation time. Now the point is that, if we want to use the cosmological observations which are based on the biased tracers of dark matter (like ISW-galaxy cross correlation function), we have to redefine the evolved bias parameter due to the dynamics of the new cosmological model. For example in Fig.(2), we plot the ration of the evolved bias to Press-Schechter bias minus one in terms of the redshift of observation. In order to find the Press-Schechter bias, we assume that the Luminous Red galaxies are typically hosted by dark matter halos of  $M \sim 10^{13} M_\odot$ . Another piece of information we need is the formation redshift of the host halos. We assume that the halo of LRGs are approximately formed in redshift where their mass variance becomes unity  $\sigma(M, z_{form}) \simeq 1$ . This condition set the formation time equal to  $z_{form} \simeq 2$  for this sample. This very rough approximation is in a good agreement from simulation data[48]. The Fig.(2) shows that the relative ratio becomes larger in low redshifts. This will have an important impact on the observations that we probe the dark matter distribution with LRG galaxies. In Fig.(3), we plot the same ratio of the evolved bias and Press-Schechter bias for SDSS, galaxy sub-sample with r-band magnitude  $18 < r < 21$  (We will discuss about the galaxy sub-samples in more detail in next section). We assume that host of this galaxies have mass of  $M \sim 10^{12} M_\odot$ . According to our estimate the formation redshift of this halos will be  $z_{form} \simeq 2.5$ . It is obvious that in the redshift of the formation, the evolved bias is the same as the Press-Schechter bias. In the next section we will show the theoretical result for ISW-galaxy correlation with emphasizing on the degeneracy of free parameter of model and dark energy clustering.

## V. GALAXY CATALOG, BIAS AND ISW-G CORRELATION

In this section we compare and show the degeneracy of dark energy models prediction for the cross correlation of ISW and galaxy angular power spectrum with bias parameter. We also discuss the importance of the *joint kernel*, introduced in this work, to deduce the effect of a dark energy model on the signal. In Fig. (4) The ISW-galaxy angular correlation function in micro-kelvin is plotted versus separation angle for  $\Lambda$ CDM model (red solid line) in comparison with the dark energy model assuming the CPL parametrization introduced in Eq.(19). Accordingly, we



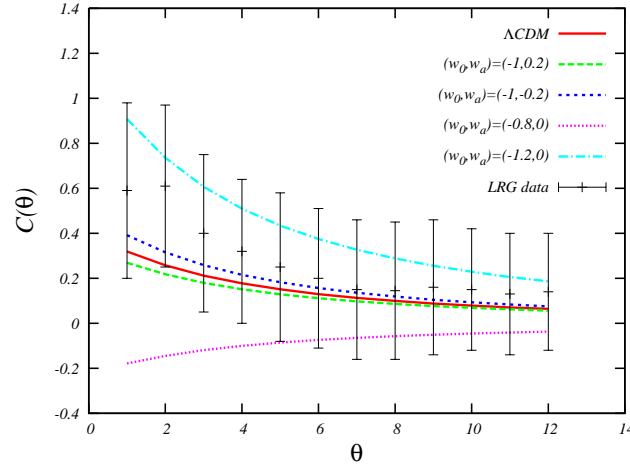


FIG. 4: The angular power of the ISW-galaxy in micro-Kelvin is plotted versus the angle of separation, for dark energy models. The red solid line indicate the  $\Lambda$ CDM, the green long-dashed line shows a dark energy model with  $(w_0, w_a) = (-1, 0.2)$ . The blue dashed line is for a model with  $(w_0, w_a) = (-1, -0.2)$ , the magenta dotted line is for equation of state  $(w_0, w_a) = (-0.8, 0)$  and cyan dashed-dotted line indicate  $(w_0, w_a) = (-1.2, 0)$ . The bias parameter is set to a constant ( $b = 1.8$ ). The data points are taken from Luminous Red Galaxy sample.

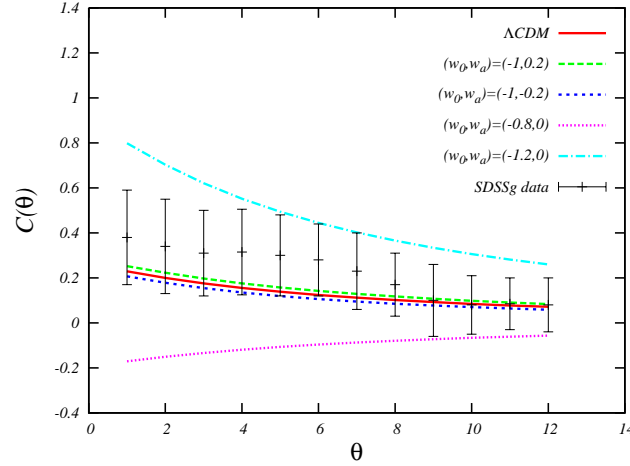


FIG. 5: The angular power of the ISW-galaxy in micro-kelvin is plotted versus the angle for dark energy models. The red solid line indicate the  $\Lambda$ CDM, the green long-dashed line shows a dark energy model with  $(w_0, w_a) = (-1, 0.2)$ . The blue dashed line is for a model with  $(w_0, w_a) = (-1, -0.2)$ , the magenta dotted line is for equation of state  $(w_0, w_a) = (-0.8, 0)$  and cyan dashed-dotted line indicate  $(w_0, w_a) = (-1.2, 0)$ . The bias parameter is set to a constant ( $b = 1.0$ ). The data points are taken from SDSS Galaxy sample.

use the combination of 4 points from parameter space of equation of state  $(w_0, w_a) = (-1, 0.2)$ ,  $(w_0, w_a) = (-1, -0.2)$ ,  $(w_0, w_a) = (-1.2, 0)$  and  $(w_0, w_a) = (-0.8, 0)$  which is studied in Fig.(1). The first three points are compatible with the Planck data (angular correlation of temperature) in combination with Baryon Acoustic Oscillation (BAO) data and SNeI data (The Joint Light-curve Analysis sample (JLA) [39] and local measurement of  $H_0$  in  $2\sigma$  confidence [40]. The last combination  $(w_0, w_a) = (-0.8, 0)$  has a  $2\sigma$  tension with the Planck data. The LRG data sample of ISW-g correlation function also shows that  $(w_0, w_a) = (-0.8, 0)$  is already ruled out with the constant bias parameter. The effect of changing the bias will be studied later in this section.

The data points in Fig. (4), are from the cross correlation of the CMB data with Luminous Red Galaxies (LRG)s which are extracted from the SDSS catalog[44]. LRGs are suitable choice as a tracer of dark matter distribution as they have a deeper redshift distribution (with a mean redshift of  $z \sim 0.5$ ) than the ordinary galaxies. Accordingly they are used to find evidence for the ISW effect previously [41, 42]. In this analysis we use the data points from [43] which is processed from "MegaZ LRG" sample [44, 45], which contains 1.5 million objects from the SDSS DR6 selected with

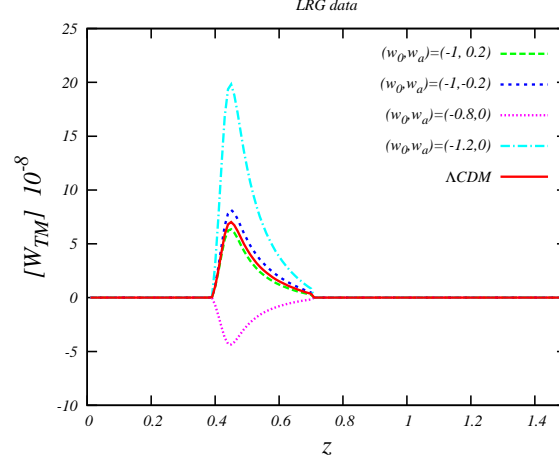


FIG. 6: The joint Kernel of ISW-galaxy  $W_{TM}$  for the Luminous Red Galaxy (LRG) survey is plotted versus redshift. The red solid line indicate the  $\Lambda$ CDM, the green long-dashed line shows a dark energy model with  $(w_0, w_a) = (-1, 0.2)$ . The blue dashed line is for a model with  $(w_0, w_a) = (-1, -0.2)$ , the magenta dotted line is for equation of state  $(w_0, w_a) = (-0.8, 0)$  and cyan dashed-dotted line indicate  $(w_0, w_a) = (-1.2, 0)$ .

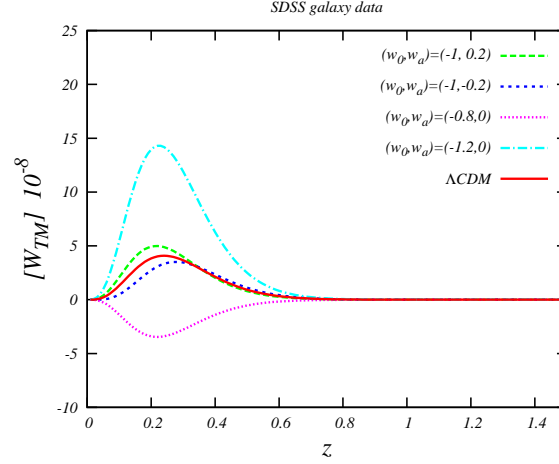


FIG. 7: The joint Kernel of ISW-galaxy  $W_{TM}$  for a sub-sample of galaxies from SDSS sub-sample is plotted versus redshift. The red solid line indicate the  $\Lambda$ CDM, the green long-dashed line shows a dark energy model with  $(w_0, w_a) = (-1, 0.2)$ . The blue dashed line is for a model with  $(w_0, w_a) = (-1, -0.2)$ , the magenta dotted line is for equation of state  $(w_0, w_a) = (-0.8, 0)$  and cyan dashed-dotted line indicate  $(w_0, w_a) = (-1.2, 0)$ .

a neural network. The theoretical curves which are plotted in Fig.(4) have the assumption of the halo-dark matter bias to be a constant ( $b = 1.8$ )[43]. The error bars in the LRG catalog are quite large in  $1\sigma$  level. Accordingly all the data points chosen from free parameter space of CPL parameterizations except  $(w_0, w_a) = (-0.8, 0)$  is compatible with ISW-galaxy data in the proposed level of confidence.

In Fig.(5), the same theoretical models are plotted in comparison of the standard model  $\Lambda$ CDM prediction. In this plot, we compare the theoretical curves with the other catalog of the galaxies taken from SDSS galaxy sample [43]. The data set is from SDSS Sixth Data Release (DR6) [46, 47]. From this catalogue a magnitude limited sub-sample is chosen as  $18 < r < 21$ , where "r is the extinction corrected SDSS calibrated model magnitude" [43]. In this case, the catalog contains almost  $3 \times 10^6$  galaxies. Using the chosen SDSS-galaxy sub-sample as a probe of ISW-g correlation, we find a more significant tension between dark energy model with equation of state of the parameter  $(w_0, w_a) = (-0.8, 0)$  and also  $(w_0, w_a) = (-1.2, 0)$ . In future galaxy surveys, where we will have more wider and deeper galaxy surveys, we will be able to constrain the dark energy equation of state more accurately. This is because the ISW-galaxy correlation is a dynamical probe of dark energy models. A probe which in the same time captures the effect of the deviation from  $\Lambda$ CDM in background (Hubble parameter) and in the level of perturbations via matter

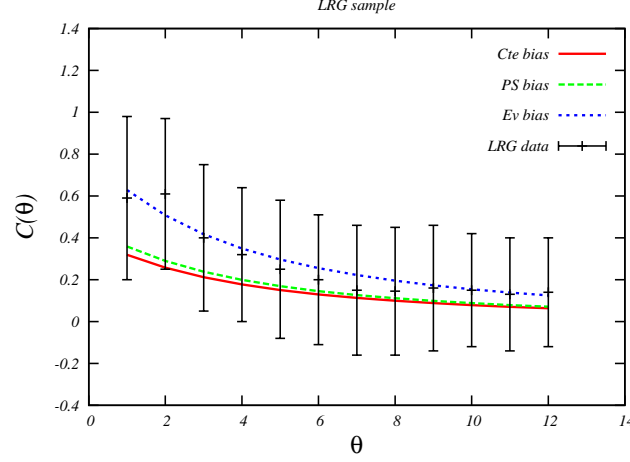


FIG. 8: The angular power of the ISW-galaxy in micro-kelvin is plotted versus the angle for  $\Lambda$ CDM model with different biases. The red solid line showed the constant bias ( $b = 1.8$ ), the green long dashed line showed the Press-Schechter bias for dark matter halo mass of  $M = 10^{13} M_{\odot}$  and the blue dashed line showed the evolved bias with the assumption of  $z_{form} = 2$ . The data points are taken from LRG sample.

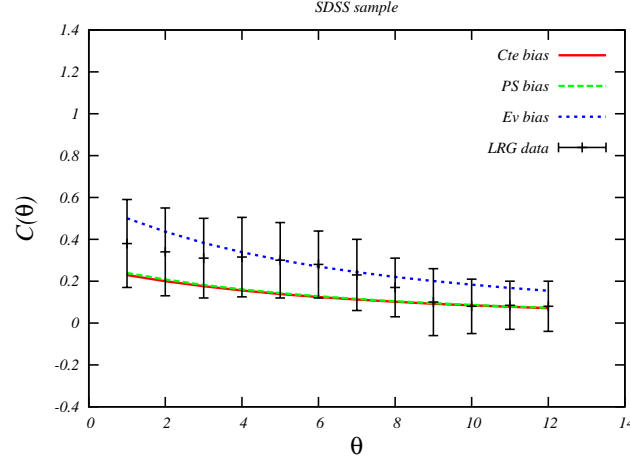


FIG. 9: The angular power of the ISW-galaxy in micro-kelvin is plotted versus the angle for  $\Lambda$ CDM model with different biases. The red solid line showed the constant bias ( $b = 1.0$ ), the green long dashed line showed the Press-Schechter bias for dark matter halo mass of  $M = 10^{12} M_{\odot}$  and the blue dashed line showed the evolved bias with assumption of  $z_{form} = 2.5$ . The data points are taken from SDSS sample.

power spectrum and growth function.

An important point to indicate here is that there is not a one to one projection between the behavior of the deviation from  $\Lambda$ CDM shown in  $Q$  parameter plotted in Fig.(1) and the signal of ISW-galaxy correlation function. This can be anticipated because the ISW-galaxy signal is not sourced only by the clustered dark energy model but it has the effect of the dark matter distribution on it as well. In order to understand this effect, in Fig.(6) and (7), we showed the evolution of joint kernel of ISW-galaxy ( $W_{TM}$ ) versus redshift for different models of dark energy. The joint kernel is defined as the multiplication of two kernels  $W_M$  and  $W_T$  as:

$$W_{TM} = W_T \times W_M \quad (39)$$

where  $W_T$  and  $W_M$  are defined as below:

$$W_M = \frac{dN}{dz} \tilde{D}(z) \quad (40)$$

where  $dN/dz$  is the galaxy distribution function defined previously and  $\tilde{D}$  indicates that the growth function is

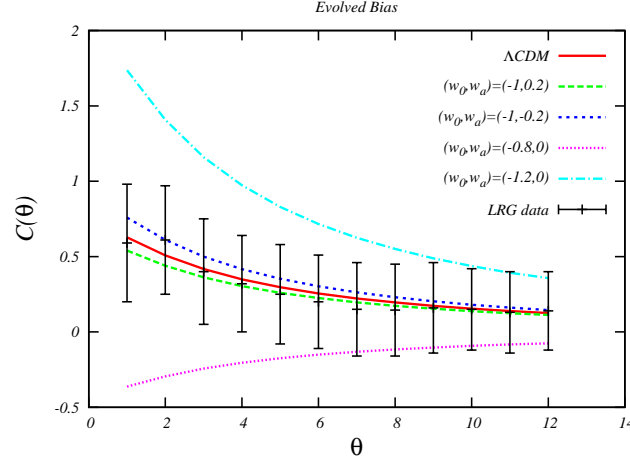


FIG. 10: The angular power of the ISW-galaxy in micro-kelvin is plotted versus the angle of separation, for dark energy models. The red solid line indicate the  $\Lambda$ CDM, the green long-dashed line shows a dark energy model with  $(w_0, w_a) = (-1, 0.2)$ . The blue dashed line is for a model with  $(w_0, w_a) = (-1, -0.2)$ , the magenta dotted line is for equation of state  $(w_0, w_a) = (-0.8, 0)$  and cyan dashed-dotted line indicate  $(w_0, w_a) = (-1.2, 0)$ . The bias is the evolved one for dark matter halos of  $M = 10^{13} M_\odot$  and  $z_{form} = 2.0$ . The data points are taken from SDSS LRG sample.

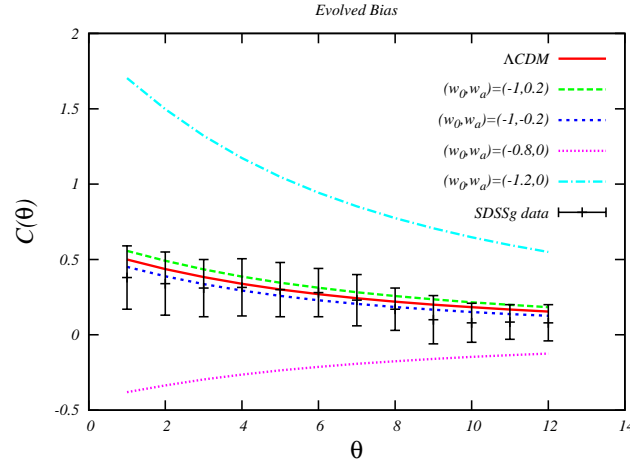


FIG. 11: The angular power of the ISW-galaxy in micro-kelvin is plotted versus the angle of separation, for dark energy models. The red solid line indicate the  $\Lambda$ CDM, the green long-dashed line shows a dark energy model with  $(w_0, w_a) = (-1, 0.2)$ . The blue dashed line is for a model with  $(w_0, w_a) = (-1, -0.2)$ , the magenta dotted line is for equation of state  $(w_0, w_a) = (-0.8, 0)$  and cyan dashed-dotted line indicate  $(w_0, w_a) = (-1.2, 0)$ . The bias is the evolved one for dark matter halos of  $M = 10^{12} M_\odot$  and  $z_{form} = 2.5$ . The data points are taken from SDSS Galaxy sample.

different from that of the standard case of  $\Lambda$ CDM.

$$W_T = 3k^{-2}(\mathcal{H}\Omega_m\tilde{D}(z)Q)_{,\eta} \quad (41)$$

where  $\eta$  is derivative with respect to conformal time. Now by comparing the Fig. (4) with Fig. (6) and (5) with Fig. (7) we will find the one to one relation between  $W_{TM}$  and the ISW-g correction function results. The distribution function of the galaxies in two catalog are so crucial that it changes the amplitude of the signal for two dark energy models with  $(w_0, w_a) = (-1, 0.2)$  and  $(w_0, w_a) = (-1, -0.2)$  for the SDSS- galaxy sample. This will have an important implication in future observations to chose the multi galaxy sub-sample to probe the dark energy as each galaxy sample probe different redshift intervals more effectively. This shows that except the evolution of dark energy model, it is important to understand the distribution of the dark matter tracers.

In following we will study the effect of dark matter halo bias on the ISW-galaxy signal. In Fig. (8), we plot the angular power of ISW-g effect for  $\Lambda$ CDM with differen biases versus angle of separation. The red solid line shows

the result using the constant bias  $b = 1.8$ . The Press Schechter bias (green long dashed line) is obtained by the assumption of  $M = 10^{13} M_{\odot}$  as the Mass of host dark matter of luminous red galaxies. The ISW-g signal which is obtained by Press-Schechter is very similar to the effect of constant bias. The blue dashed line shows the ISW-g signal with evolved bias obtained from Eq.(38) with assumption of  $z_{form} = 2.0$  [48]. The  $\Lambda$ CDM fit with evolved bias improved the fit by  $\Delta\chi^2 \simeq 2.1$ .

It is interesting to note that there are studies [28, 43, 49] showing that the data are  $\sim 1\sigma$  to  $\sim 2\sigma$  is higher than the standard model prediction. The same is obtained from stacking of the voids and clusters [50, 51]. In [29], they used the lensing data in order to constrain the bias parameter which shows that the bias is not constant in all range of integration of ISW-g signal. The same can be stated here that the evolving bias decrease the tension of data and  $\Lambda$ CDM model.

In Fig. (5), we plot the angular power of ISW-g effect for  $\Lambda$ CDM with differen biases versus angle of separation, this time for the SDSS galaxy sample. The red solid line shows the result using the constant bias  $b = 1.0$ . The Press Schechter bias (green long dashed line) is obtained by the assumption of  $M = 10^{12} M_{\odot}$  as the Mass of host dark matter of luminous red galaxies. The ISW-g signal which is obtained by Press-Schechter is very similar to the effect of constant bias here as well. The blue dashed line shows the ISW-g signal with evolved bias obtained from Eq.(38) with assumption of  $z_{form} = 2.5$  [52]. The  $\Lambda$ CDM fit with evolved bias improved the fit by  $\Delta\chi^2 \simeq 1.9$ . Once more this result shows that the evolved bias could be a probable solution to the discrepancy of  $\Lambda$ CDM and observational data.

Now we come back to study of the dark energy clustering with the evolved bias term consideration. In Fig.(10) and Fig.(11) we study the effect of the evolved bias on the signal of ISW-g. As we anticipate from Fig.(2) and Fig.(3), the evolved bias is almost twice the Press-Schechter bias in intermediate redshifts where two catalogs of LRG and SDSS galaxies are most effective. Accordingly taking in to account of the evolved bias parameter can constrain the equation of state parameters ( $w_0, w_a$ ) more tightly. This is very promising that the future more accurate data of ISW and galaxy cross correlation by adding the right bias term can pin down the equation of state of dark energy.

## VI. CONCLUSION AND FUTURE REMARKS

The accelerated expansion of the Universe is one of the great mysterious of modern cosmology. One way to address this problem is measuring the possible deviations from cosmological constant prediction for the model. The phenomenological parametrization of equation of state of cosmic fluid with a time dependent equation of state  $w = w(z)$  is one way to address this problem via comparison with the cosmological data driven from geometrical and dynamical observations. One of the most prominent cosmological observations is ISW -galaxy correlation which probes the geometry and dynamic of the cosmological models in different redshift and in an integrated way. In this work we show that the deviation of the cross correlation of the ISW-g signal from standard case is not proportional to deviation of the model in Poisson equation, (parameterized in  $Q$ -parameter), while it depend on the dynamical parameter of the ISW-g correlation and the distribution of the galaxies. Accordingly we conclude that different galaxy catalogs with different selection functions can probe dark energy models in different redshifts. We show how the signal of ISW-galaxy correlation function depend on the joint kernel function ( $W_{TM}$ ) which is obtained from dynamical parameters. The dynamical parameters are the growth function, the ISW kernel  $W_T$  and the distribution of galaxies  $dN/dz$ .

The other important point we conclude is the degeneracy of the two different physics on the ISW-g signal. On one hand, we have the deviation from  $\Lambda$ CDM which affect the kernels and matter power spectrum respectively which can change the signal of the  $ISW - g$  correlation function. On the other is the bias parameter, the relation of luminous matter with the underlying distribution of dark matter. In this work we just assume the dark matter halo bias, we showed that the there is a degeneracy between two physics.

In this direction we study the ISW-g signal with constant bias, the Press-Schechter bias and the evolved bias. We argue that the more accurate bias is the evolved one as the observation and formation time of dark matter halos does not coincide. We show that the evolved bias parameter is a probable solution to resolve the reported  $1\sigma$  up to  $2\sigma$  tension of the  $\Lambda$ CDM model with observational signals. This result is in agreement with recent work by [29] that assume evolved bias which is fixed with lensing data. We also conclude that using the evolved bias tightens the constraint on the equation of state of a dark energy. The forecast of the constrained on the equation of state of dark energy can be an extension to this work by assuming the evolved bias. The future galaxy surveys will extend the depth and width of the galaxy maps and the constrained on dark energy will be improved accordingly. On the other hand the independent measurement of the bias parameter will have a crucial importance to pin down the dark matter

- baryonic segment of the problem and to improve the constraints on dark energy.

### Acknowledgments

We would like to thank Farshid Deylami for many discussions and comments on the work. Also we thank Yashar Akrami, Nima Khosravi and Sohrab Rahvar for insightful comments.

- 
- [1] A. G. Riess *et al.* [Supernova Search Team Collaboration], “Observational evidence from supernovae for an accelerating universe and a cosmological constant,” *Astron. J.* **116** (1998) 1009 [astro-ph/9805201].
  - [2] S. Perlmutter *et al.* [Supernova Cosmology Project Collaboration], “Measurements of Omega and Lambda from 42 high redshift supernovae,” *Astrophys. J.* **517** (1999) 565 [astro-ph/9812133].
  - [3] E. Komatsu *et al.* [WMAP Collaboration], “Seven-Year Wilkinson Microwave Anisotropy Probe (WMAP) Observations: Cosmological Interpretation,” *Astrophys. J. Suppl.* **192**, 18 (2011) [arXiv:1001.4538 [astro-ph.CO]].
  - [4] P. A. R. Ade *et al.* [Planck Collaboration], “Planck 2013 results. XVI. Cosmological parameters,” arXiv:1303.5076 [astro-ph.CO].
  - [5] M. Tegmark *et al.* [SDSS Collaboration], “Cosmological parameters from SDSS and WMAP,” *Phys. Rev. D* **69**, 103501 (2004) [astro-ph/0310723].
  - [6] S. M. Carroll, “The Cosmological constant,” *Living Rev. Rel.* **4**, 1 (2001) [astro-ph/0004075].
  - [7] S. i. Nojiri and S. D. Odintsov, “Introduction to modified gravity and gravitational alternative for dark energy,” *eConf C 0602061*, 06 (2006) [Int. J. Geom. Meth. Mod. Phys. **4**, 115 (2007)] [hep-th/0601213].
  - [8] T. P. Sotiriou and V. Faraoni, “f(R) Theories Of Gravity,” *Rev. Mod. Phys.* **82**, 451 (2010) [arXiv:0805.1726 [gr-qc]].
  - [9] A. De Felice and S. Tsujikawa, “f(R) theories,” *Living Rev. Rel.* **13**, 3 (2010) [arXiv:1002.4928 [gr-qc]].
  - [10] T. Clifton, P. G. Ferreira, A. Padilla and C. Skordis, “Modified Gravity and Cosmology,” *Phys. Rept.* **513**, 1 (2012) [arXiv:1106.2476 [astro-ph.CO]].
  - [11] P. J. E. Peebles and B. Ratra, “The Cosmological constant and dark energy,” *Rev. Mod. Phys.* **75**, 559 (2003) [astro-ph/0207347].
  - [12] S. Baghran and S. Rahvar, “Structure formation in f(R) gravity: A distinguishing probe between the dark energy and modified gravity,” *JCAP* **1012**, 008 (2010) [arXiv:1004.3360 [astro-ph.CO]].
  - [13] N. Mirzatuny, S. Khosravi, S. Baghran and H. Moshafi, “Simultaneous effect of modified gravity and primordial non-Gaussianity in large scale structure observations,” *JCAP* **1401**, 019 (2014) [arXiv:1308.2874 [astro-ph.CO]].
  - [14] S. Baghran, S. Tavasoli, F. Habibi, R. Mohayaee and J. Silk, “Unraveling the nature of Gravity through our clumpy Universe,” *Int. J. Mod. Phys. D* **23**, no. 12, 1442025 (2014) [arXiv:1411.7010 [astro-ph.CO]].
  - [15] D. J. Eisenstein *et al.* [SDSS Collaboration], “Detection of the baryon acoustic peak in the large-scale correlation function of SDSS luminous red galaxies,” *Astrophys. J.* **633**, 560 (2005) [astro-ph/0501171].
  - [16] S. Cole *et al.* [2dFGRS Collaboration], “The 2dF Galaxy Redshift Survey: Power-spectrum analysis of the final dataset and cosmological implications,” *Mon. Not. Roy. Astron. Soc.* **362**, 505 (2005) [astro-ph/0501174].
  - [17] W. J. Percival, S. Cole, D. J. Eisenstein, R. C. Nichol, J. A. Peacock, A. C. Pope and A. S. Szalay, “Measuring the Baryon Acoustic Oscillation scale using the SDSS and 2dFGRS,” *Mon. Not. Roy. Astron. Soc.* **381**, 1053 (2007) [arXiv:0705.3323 [astro-ph]].
  - [18] W. J. Percival *et al.* [SDSS Collaboration], “Baryon Acoustic Oscillations in the Sloan Digital Sky Survey Data Release 7 Galaxy Sample,” *Mon. Not. Roy. Astron. Soc.* **401**, 2148 (2010) [arXiv:0907.1660 [astro-ph.CO]].
  - [19] A. Vikhlinin *et al.*, “Chandra Cluster Cosmology Project III: Cosmological Parameter Constraints,” *Astrophys. J.* **692**, 1060 (2009) [arXiv:0812.2720 [astro-ph]].
  - [20] L. Fu *et al.*, “Very weak lensing in the CFHTLS Wide: Cosmology from cosmic shear in the linear regime,” *Astron. Astrophys.* **479**, 9 (2008) [arXiv:0712.0884 [astro-ph]].
  - [21] U. Seljak *et al.* [SDSS Collaboration], “Cosmological parameter analysis including SDSS Ly-alpha forest and galaxy bias: Constraints on the primordial spectrum of fluctuations, neutrino mass, and dark energy,” *Phys. Rev. D* **71**, 103515 (2005) [astro-ph/0407372].
  - [22] R. K. Sachs and A. M. Wolfe, “Perturbations of a cosmological model and angular variations of the microwave background,” *Astrophys. J.* **147** (1967) 73 [Gen. Rel. Grav. **39** (2007) 1929].
  - [23] K. M. Huffenberger, U. Seljak and A. Makarov, *Phys. Rev. D* **70**, 063002 (2004) [astro-ph/0404545].
  - [24] P. A. R. Ade *et al.* [Planck Collaboration], “Planck 2015 results. XXI. The integrated Sachs-Wolfe effect,” arXiv:1502.01595 [astro-ph.CO].
  - [25] R. G. Crittenden and N. Turok, “Looking for Lambda with the Rees-Sciama effect,” *Phys. Rev. Lett.* **76**, 575 (1996) [astro-ph/9510072].
  - [26] S. Boughn and R. Crittenden, “A Correlation of the cosmic microwave sky with large scale structure,” *Nature* **427** (2004) 45 [astro-ph/0305001].
  - [27] P. S. Corasaniti, T. Giannantonio and A. Melchiorri, *Phys. Rev. D* **71**, 123521 (2005) [astro-ph/0504115].



- [28] S. Ho, C. Hirata, N. Padmanabhan, U. Seljak and N. Bahcall, “Correlation of CMB with large-scale structure: I. ISW Tomography and Cosmological Implications,” *Phys. Rev. D* **78**, 043519 (2008) [arXiv:0801.0642 [astro-ph]].
- [29] S. Ferraro, B. D. Sherwin and D. N. Spergel, “WISE measurement of the integrated Sachs-Wolfe effect,” *Phys. Rev. D* **91**, no. 8, 083533 (2015) [arXiv:1401.1193 [astro-ph.CO]].
- [30] L. Amendola and S. Tsujikawa, *Dark Energy: Theory and Observations*, Cambridge University Press, 2010.
- [31] M. Chevallier and D. Polarski, “Accelerating universes with scaling dark matter,” *Int. J. Mod. Phys. D* **10**, 213 (2001) [gr-qc/0009008].
- [32] E. V. Linder, “Exploring the expansion history of the universe,” *Phys. Rev. Lett.* **90**, 091301 (2003) [astro-ph/0208512].
- [33] J. M. Bardeen, J. R. Bond, N. Kaiser and A. S. Szalay, “The Statistics of Peaks of Gaussian Random Fields,” *Astrophys. J.* **304**, 15 (1986).
- [34] A. A. Berlind and D. H. Weinberg, “The Halo occupation distribution: Towards an empirical determination of the relation between galaxies and mass,” *Astrophys. J.* **575**, 587 (2002) [astro-ph/0109001].
- [35] W. H. Press and P. Schechter, “Formation of galaxies and clusters of galaxies by selfsimilar gravitational condensation,” *Astrophys. J.* **187**, 425 (1974).
- [36] J. N. Fry and E. Gaztanaga, “Biasing and hierarchical statistics in large scale structure,” *Astrophys. J.* **413**, 447 (1993) [astro-ph/9302009].
- [37] L. Hui and K. P. Parfrey, “The Evolution of Bias: Generalized,” *Phys. Rev. D* **77**, 043527 (2008) [arXiv:0712.1162 [astro-ph]].
- [38] K. Parfrey, L. Hui and R. K. Sheth, “Scale-dependent halo bias from scale-dependent growth,” *Phys. Rev. D* **83**, 063511 (2011) [arXiv:1012.1335 [astro-ph.CO]].
- [39] M. Betoule *et al.* [SDSS Collaboration], *Astron. Astrophys.* **568**, A22 (2014) [arXiv:1401.4064 [astro-ph.CO]].
- [40] P. A. R. Ade *et al.* [Planck Collaboration], ‘Planck 2015 results. XIII. Cosmological parameters,’ arXiv:1502.01589 [astro-ph.CO].
- [41] R. Scranton *et al.* [SDSS Collaboration], “Physical evidence for dark energy,” astro-ph/0307335.
- [42] N. Padmanabhan, C. M. Hirata, U. Seljak, D. Schlegel, J. Brinkmann and D. P. Schneider, “Correlating the CMB with luminous red galaxies: The Integrated Sachs-Wolfe effect,” *Phys. Rev. D* **72**, 043525 (2005) [astro-ph/0410360].
- [43] T. Giannantonio, R. Scranton, R. G. Crittenden, R. C. Nichol, S. P. Boughn, A. D. Myers and G. T. Richards, “Combined analysis of the integrated Sachs-Wolfe effect and cosmological implications,” *Phys. Rev. D* **77**, 123520 (2008) [arXiv:0801.4380 [astro-ph]].
- [44] C. Blake, A. Collister, S. Bridle and O. Lahav, “Cosmological baryonic and matter densities from 600,000 SDSS Luminous Red Galaxies with photometric redshifts,” *Mon. Not. Roy. Astron. Soc.* **374**, 1527 (2007) [astro-ph/0605303].
- [45] A. Collister *et al.*, “MegaZ-LRG: A photometric redshift catalogue of one million SDSS Luminous Red Galaxies,” *Mon. Not. Roy. Astron. Soc.* **375**, 68 (2007) [astro-ph/0607630].
- [46] J. K. Adelman-McCarthy *et al.* [SDSS Collaboration], “The Sixth Data Release of the Sloan Digital Sky Survey,” *Astrophys. J. Suppl.* **175**, 297 (2008) [arXiv:0707.3413 [astro-ph]].
- [47] D. G. York *et al.* [SDSS Collaboration], “The Sloan Digital Sky Survey: Technical Summary,” *Astron. J.* **120**, 1579 (2000) [astro-ph/0006396].
- [48] S. Masaki, C. Hikage, M. Takada, D. N. Spergel and N. Sugiyama, “Understanding the nature of luminous red galaxies (LRGs): Connecting LRGs to central and satellite subhalos,” *Mon. Not. Roy. Astron. Soc.* **433**, 3506 (2013) [arXiv:1211.7077 [astro-ph.CO]].
- [49] T. Goto, I. Szapudi and B. R. Granett, “Cross-correlation of WISE Galaxies with the Cosmic Microwave Background,” *Mon. Not. Roy. Astron. Soc.* **422** (2012) L77 [arXiv:1202.5306 [astro-ph.CO]].
- [50] B. R. Granett, M. C. Neyrinck and I. Szapudi, “An Imprint of Super-Structures on the Microwave Background due to the Integrated Sachs-Wolfe Effect,” *Astrophys. J.* **683**, L99 (2008) [arXiv:0805.3695 [astro-ph]].
- [51] P. A. R. Ade *et al.* [Planck Collaboration], “Planck 2013 results. XIX. The integrated Sachs-Wolfe effect,” *Astron. Astrophys.* **571**, A19 (2014) [arXiv:1303.5079 [astro-ph.CO]].
- [52] P. G. van Dokkum *et al.*, “The Assembly of Milky Way-like Galaxies Since  $z = 2.5$ ,” *Astrophys. J.* **771**, L35 (2013) [arXiv:1304.2391 [astro-ph.CO]].